Textural ageing in *Pygoscelis antarctica* (Aves, Sphenisciformes): a new comparative scale for penguin bones

Carolina Acosta Hospitaleche & Mariana J. B. Picasso

CONICET, División Paleontología Vertebrados, Museo de La Plata. Paseo del Bosque s/n B1900FWA, La Plata, Facultad de Ciencias Naturales y Museo, Universidad Nacional de La Plata, Argentina — Corresponding author: acostacaro@fcnym.unlp.edu.ar

Abstract

Textural ageing is a technique that recognizes the bone texture as a clear indicator of the post-natal ontogenetic stages in birds. Although it was only tested in a few groups of birds, the results obtained in the pioneer works were widely applied. Though convinced of the effectiveness of this technique, we also believe that given the variability that exists between birds, its application should be done using a reliable comparative scale. In this contribution, a post-natal ontogenetic series for *Pygoscelis antarctica* was built to analyze the textural ageing in penguins. We used the same descriptive terms to characterize each texture as in previous contributions, to make the scales comparable to each other. The variations were standardized, and a new comparative scale for penguins was proposed.

Key words

Spheniscidae, seabirds, Antarctica, comparative textures, post-natal ontogeny.

Introduction

Although embryological development of birds skeleton has been and continues to be widely studied (e.g. Fujioka, 1955; Rogulska, 1962; Starck, 1993; Pourlis *et al.*, 1998; Pourlis & Antonopoulus, 2014), post-natal ontogeny has not been intensively investigated, except for a few works that focused on general morphology (Hogg, 1980; Cane, 1993; Picasso, 2012; Picasso & Barbeito, 2018; Piro & Acosta Hospitaleche, 2018; Sosa & Acosta Hospitaleche, 2017) and histology (Müller & Streicher, 1989; de Margerie *et al.*, 2004; Knoll *et al.*, 2018), among others. The study of variations in bones morphology along post-natal ontogeny has not been substantially addressed in the field of ornithology. The knowledge of these post-natal ontogenetic changes is a crucial point in anatomical studies, allowing the understanding and interpretation of the observed variations.

Pioneering work on post-natal ontogeny of the Canada goose demonstrated that the bone texture correlates with age and constitutes a clear indicator of the ontogenetic stages. This technique used to determine the ontogenetic stage was called as textural ageing (Tumarkin-Deratzian *et al.*, 2006). It is a non-invasive or destructive technique, independent of size, and based on a macroscopic examination of the bones. Due to the importance of the age determination of a specimen before the addressing of any other kind of study in paleontology and archeology, the contribution of Tumarkin-Deratzian *et al.* (2006) quickly became a publication of reference. Since then, new complete ontogenetic series were only evaluated for a few taxa (Watanabe & Matsuoka, 2013; Acosta Hospitaleche *et al.*, 2017; Watanabe, 2017, 2018), and many studies based the age establishment on the observations made on the Anatidae *Branta canadensis* (Tumarkin-Deratzian *et al.* 2006).

Three contributions summarize the history of the textural aging in ornithology. In the first one, seven types of osteological textures were proposed to describe the vari-

ations in the Anatidae *Branta canadiensis* (Tumarkin-Deratzian *et al.*, 2006). In the second study, five textures were described for the Ardeidae *Ardea cinerea* (Watanabe & Matsuoka, 2013). The novelty, in this case, was that each bone was described using different combinations of textures and defining patterns. And finally, eight intergrading types were proposed to characterize the textures of *Calonectris leucomelas* (Procellariidae), *Phalacrocorax capillatus* (Phalacrocoracidae), *Larus crassirostris* (Laridae) and *Cerorhinca monocerata* (Alcidae) (Watanabe, 2018).

The differences in the results of the contributions mentioned above would indicate that it is not possible to reliably extrapolate features of textures from one taxonomic group to another. That is, each order or family of birds would have its own characteristics to define the different ontogenetic stages, probably related to the type of growth and maturation rate. Thus, comparative data are still limited, and the taxonomic variations in the ossification are still unknown.

Penguins (Aves, Sphenisciformes), for instance, constitute a group of seabirds with extreme modifications in their skeleton linked to their adaptation for diving. The pneumatization has almost been lost, and bones are dense, compact, and thick-walled, with marked pachyostosis (Houssaye, 2009). Penguins are wing-propelled diving birds, with short and flattened bones that fuse turning wings into flippers. Their legs that serve as rudders have short and broad elements, like the massively built tarsometatarsus. All these modifications make penguins skeleton completely different from other groups of birds regarding their resistance and preservability.

Penguins are particular among birds not only for their skeletal modification but also for their slow evolutive rates. This is evident in their morphologically conservative pattern and their higher greater taxonomic longevities compared to continental birds (Acosta Hospitaleche, 2006). This could differentially affect the ossification of their bones. A brief macroscopic description of humeri belonging to a post-natal ontogenetic series was provided as comparative material by Acosta Hospitaleche *et al.* (2017). However, data about textural ageing are still insufficient.

Most of the fossil penguins exhibit an extensive record, that includes disarticulated and fragmented elements in a high proportion. Since these deposits correspond to sites where the reproductive colonies were settled down, or to places near to the breeding colonies, individuals of different ages are usually collected. A correct interpretation of these assemblages and the genesis of the deposits requires proper allocation of the specimens into the ontogenetic stages. Indeed, the recognition of the ontogenetic stage of the specimens is a prior requirement of any systematic, paleobiologic, and taphonomic approach. For that reason, the characterization of textural ageing that allows accurate identification of chicks, juveniles, and adults is extremely important.

The main goal of the present contribution is the analysis of the textural ageing in penguins and the standardization of the variations along the post-natal ontogeny. We built a post-natal ontogenetic series composed of skeletons of *Pygoscelis antarctica*. After examination of the superficial textures of the elements of the wings and legs, we proposed a comparative scale for penguins. Also, as the bone morphology of juveniles differs from those of adults, we also make a qualitative description of the bones of non-adult penguins.

Material and methods

Specimens collection. The fore and hind limbs of 35 specimens of *Pygoscelis antarctica* from breeding colonies and others housed in the museum collections were studied. Non-adult and adult specimens were collected from the breeding colonies after dying from natural causes, according to current international regulations. After the decomposition of the soft tissues, carcasses were washed with non-abrasive or erosive substances to remove soft tissue remains. All these specimens are housed in the Ornithology Section of the Vertebrate Zoology Division (MLP-O) and in the osteological collection of the Vertebrate Paleontology Division (MLP) of the Museo de La Plata, Argentina. Adults and non-adults specimens previously housed in MLP collections were also studied.

Ages. Individuals were allocated into three age categories: chicks ($n=21$: MLP-O 787, MLP-O 788, MLP-O 790, MLP-O 792, MLP-O 793, MLP-O 795, MLP-O 796, MLP-O 799, MLP-O 805, MLP-O 809, MLP-O 810, MLP-O 811, MLP-O 812, MLP-O 817, MLP-O 14945, MLP-O 14946, MLP-O 14947, MLP-O 14948, MLP-O 14949, MLP-O 14950, MLP-O 14951), juveniles ($n=4$: MLP-O 80, MLP-O 791, MLP-O 806, MLP-O 807), and adults ($n=10$: MLP 37, MLP 470, MLP 687, MLP 930, MLP-O 14717, MLP-O 14737, MLP-O 14916, MLP-O 14952, MLP-O 15191, MLP-O 15417). The criteria for distinguishing non-adult stages were as follows: Chicks groups the newborn penguins to those losing their downy feathers for their first set of waterproof feathers (up to four months). At this point, they are considered juveniles (from four months to about four years) until their sexual maturation (starting in the fourth year). The date of birth and death for each specimen was obtained from the monitoring program of the Instituto Antártico Argentino (IAA).

Texture and bone descriptions. Observations on textures and bones shape were conducted with naked eyes, a hand lens, and a stereoscopic microscope with magnifications of $\times 10-40$. Only differences between the bones of different categories were highlighted. Adult bones were not described here since literature can be consulted for this topic (see Waterston & Geddes, 1910; Bannasch, 1994; Acosta Hospitaleche, 2004).

Descriptions of the textures were arranged as follows: proximal end, shaft, and distal end of the *facies cranialis*

first, and then for the *facies caudalis* (for each bone of chicks, juveniles, and adults, following B<small>AUMEL</small> & W<small>IT</small>-<small>MER</small>, 1993). Specific terms for the description of the textures agree with previous authors (T<small>UMARKIN</small>- D<small>ERATZIAN</small> *et al*., 2006; W<small>ATANABE</small> & M<small>ATSUOKA</small>, 2013; W<small>ATANABE</small>, 2018) and are defined in the texture description section of the results. Particular specimens were mentioned along with the descriptions only when variations were detected.

Photographs of humerus, radius, ulna, carpometacarpus, femur, tibiotarsus, and tarsometatarsus were taken by Bruno Pianzola in the laboratories of the Museo de La Plata with a Nikon camera. In all the cases, the focal distance, the angle, and intensity of light were the same to prevent issues of variation in the surface texture.

Results

Description of the sub-adult bones

Wing. Chicks were represented by skeletons with unfused and barely ossified elements (Fig. 1). The humerus varies from a quadrangular and flat shape in newborns (Fig. 1A) to a slight curvature insinuated in the shaft and a widened distal end in two months old chicks (Fig. 1B). In the middle of this spectrum, the humerus only increases in size. The youngest juveniles (Fig. 1C) are slightly smaller than adults, and the oldest juveniles present all the morphological features that characterize the adults, including the size and the completely ossified ends. The main difference is the texture of the superficial bone (see next section).

In the next segment of the wing, the ulna is unrecognizable from the radius, at least in the youngest chicks of a few days old (Fig. 1A). Only in chicks older than two months, the radius and ulna acquire a different configuration (Fig. 1B). The oldest chicks present a widened ulna regarding the radius. The configuration of the radius and ulna in juveniles is similar to that found in adults (Fig. 1C). However, the surface of these bones is rougher in juveniles than on adults.

In chicks, the carpometacarpus is represented by two flattened and rectangular elements, similar to the ulna and radius (Fig. 1A, B). This bone comprises two separate elements: the metacarpal major and the metacarpal minor, still unfused. An increment in the size of the carpometacarpus is noticed from newborns to the largest chicks, and in the juveniles, the metacarpals are partially fused (Fig. 1C). The suture between the metacarpals major and minor is visible in the smallest juveniles, and it disappears in the largest ones.

Leg. Bones of the leg differ among chicks in their configuration (Fig. 2). In newborns chicks (Fig. 2A), the femur is distinguishable from the tibiotarsus only because of its shorter length. The diaphysis of both elements is cylindrical, and the ends are not yet ossified. In larger chicks (Fig. 2B), the femur is barely ossified, and the *fossa poplitea* is represented by a shallow depression. On
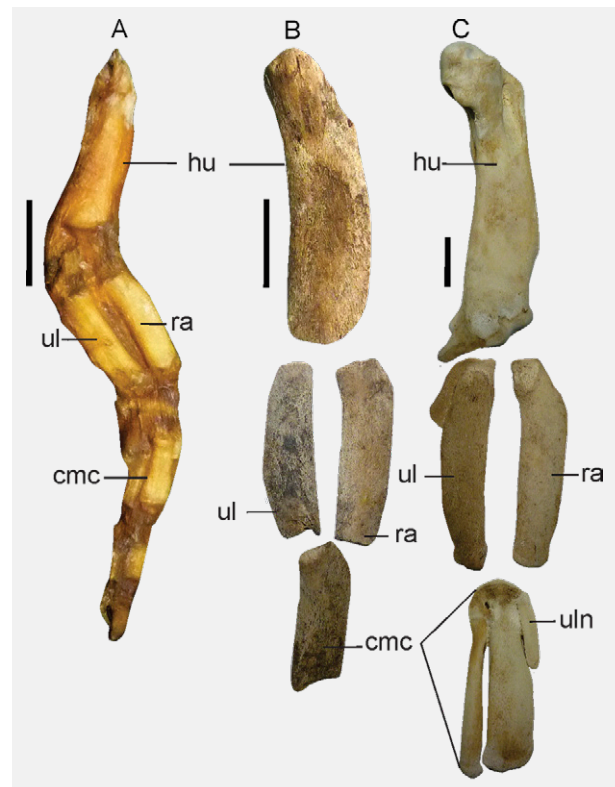

Fig. 1. General morphology of the left wing bones in cranial view: (A) Newborn chick (MLP-O 795), (B) Chick of approximately two months old (MLP-O 810), (C) Juvenile (MLP 791-O). Abbreviations: cmc: carpometacarpus, hu: humerus, ra: radius, ul: ulna, uln: ulnare. Scale bar: 5 mm.

the contrary, the tibiotarsus presents a better-defined *sulcus extensorius*.

The femur acquires the adult size in juveniles (Fig. 2C), but the proximal and distal ends are not completely ossified and fused to the shaft. The tibiotarsus presents a similar condition, with both ends free in the youngest juveniles.

The fibula is not attached to the tibiotarsus in any subadult specimen, but it ossifies as a separate element. Only in the adults the elements that constitute the tibiotarsus are completely fused to each other and attached to the fibula.

The tarsometatarsus of newborns (Fig. 2A) is formed by the three free metatarsals, not fused yet, and morphologically indistinguishable from each other. In larger chicks (Fig. 2B) the metatarsals acquire a differential development, with the third metatarsal larger than the second and fourth.

In juveniles (Fig. 2C), the metatarsals are fused, but the sutures are still visible. The fusion is complete, and the sutures disappear in adults.

Textures description

We use the following terms to describe the textures: Pores are openings of different sizes (tiny, small, large),
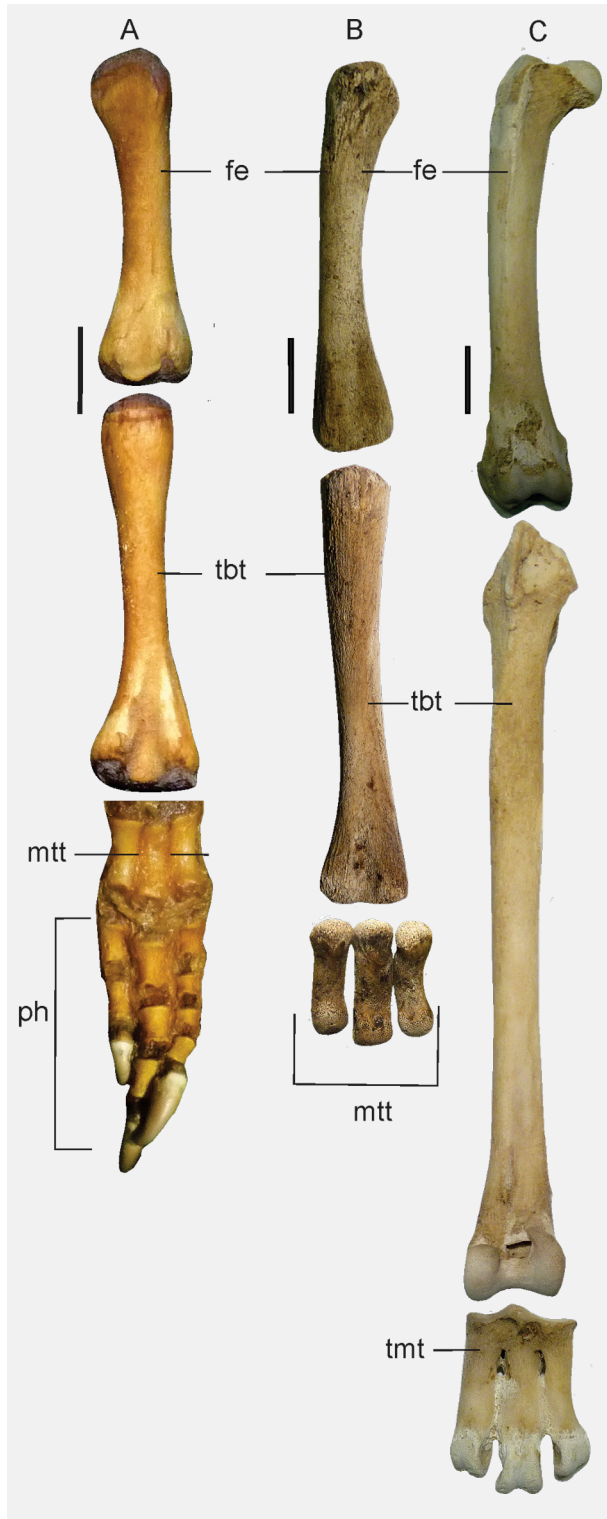
Fig. 2. General morphology of the right leg bones in cranial view: (A) Newborn chick (MLP-O 795), (B) Chick of approximately two months old (MLP-O 810), (C) Juvenile (MLP-O 791). Abbreviations: fe: femur, mtt: metatarsals, tbt: tibiotarsus, tmt: tarsometatarsus, ph: phalanges. Scale bar: 5 mm.

and shapes (elongated, sub-rounded, rounded) that can be isolated, disperse, or aligned on rows. Pores distributed along the complete area constitute a porous surface, and are considered closed when a thin layer of bone is oblite-

rating them. Foramina are several pores usually from the same size and shape. Dimples are openings larger than pores that appear isolated or in a small number, probably related to the blood vessel or nerves passage.

Furrows or grooves are a group of wide and elongated hollows (short, long), separated by osseous crests. When these furrows are very tight and narrow, and therefore the crests between them are also close to each other, we call them striations. Stretch marks are thinner and weaker lines that appear in groups, something similar is a wrinkle, although it appears isolated. All these elongated structures can be aligned to the central axis of the shaft, and parallel or oblique to the margins of the shaft.

We refer to a smooth texture when the surface is not covered by pores and furrows, due to the main ossification degree. Silky was reserved for glossy surfaces, whereas bright was used when this condition was even more pronounced. Contrarily, the rough texture is used for a surface without pores and furrows but not silky at all. A fibrous surface implies the presence of a weak and narrow striation.

Humerus

Facies cranialis. In **chicks,** the proximal end is covered by large pores, that join each other constituting short furrows (Fig. 3A). The shaft has a similar texture with large and oval pores distributed in patches (Fig. 3B), and the distal end has parallel striations that become sub-parallel and converge toward the shaft. It can be observed here the same pattern of pores (Fig. 3C); striations turn into furrows, which are wider and irregularly arranged in MLP-O 796.

In **juveniles,** the proximal end is covered by small, rounded and densely packaged pores homogeneously distributed (Fig. 3D). Tiny and isolated pores are between the longitudinal and parallel striations in the middle of the shaft (Fig. 3E). The stretch marks and pores are narrower and tighter toward the *margo ventralis* than to the *margo dorsalis*. At the middle of the diaphysis the texture is a bit rougher. The distal end is covered by a few number of variable-sized pores which are sparsely distributed, with interspersed smoother areas (Fig. 3F).

In **adults,** toward the ends, the isolated dimples are more pronounced, but most of the surface is smooth and without pores (Fig. 3G). The shaft is also smooth and presents few and tiny isolated and obliterated pores (Fig. 3H), and finally, the distal end is as smooth as the other areas in this surface, and present a few and tiny pores (Fig. 3I).

Facies caudalis. In **chicks**, the proximal end develops elongated pores that merge and form open furrows converging toward the shaft (Fig. 3J). The shaft seems a little more ossified, and a weak layer of bone covers the surface. Pores are smaller and less densely distributed in comparison with the ends (Fig. 3K). Different zones with a thin and barely furrowed bony layer are distinguished
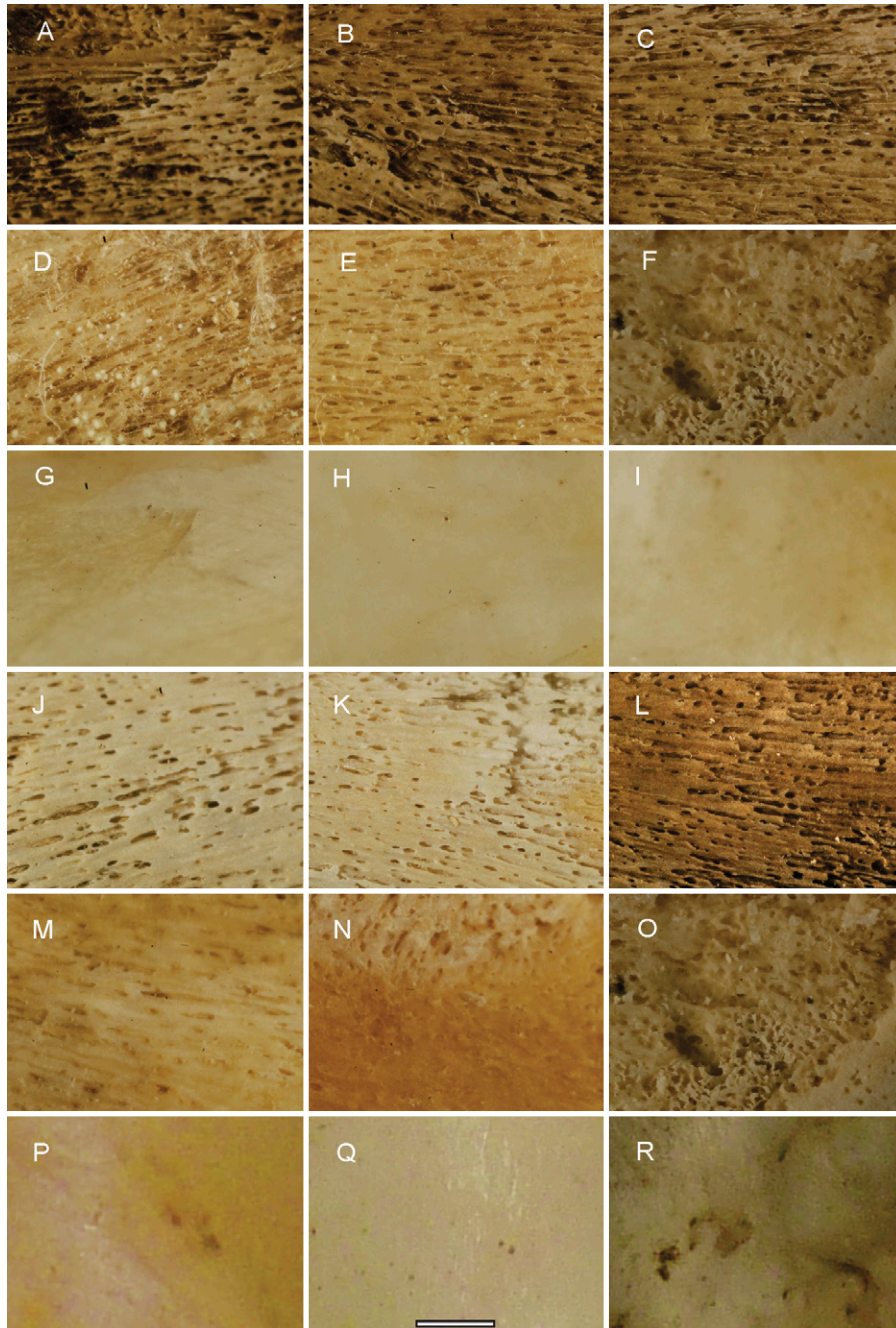
Fig. 3. Humerus textures in chicks (A−C, J−L), juveniles (D−F, M−O), and adults (D−F, P−Q). In all the cases, bones are oriented with the proximal end at the left: (A) proximal end in cranial view (MLP-O 810), (B) shaft in cranial view (MLP-O 810), (F) distal end in caudal view (MLP-O 787), (G) proximal end in cranial view (MLP 470), (H) shaft in cranial view (MLP 470), (I) distal end in cranial view (MLP 470), (J) proximal end in caudal view (MLP-O 817), (K) shaft in caudal view (MLP-O 817), (L) distal end in caudal view (MLP-O 787), (M) proximal end in caudal view (MLP-O 791), (N) shaft in caudal view (MLP-O 791), (O) distal end in caudal view (MLP-O 791), (P) proximal end in caudal view (MLP470), (Q) shaft in caudal view (MLP 470), distal end in caudal view (MLP 470). Scale bar: 1 mm.

in MLP-O 805, together with isolated dimples and irregular furrows. These marks transform into wider and open furrows without pores in MLP-O 796. The distal end is similar to the proximal one, although the furrows are denser and pores are well delimited (Fig. 3L).

In **juveniles**, the caudal face of the proximal end is a little more ossified than the cranial area, and the furrows are narrower (Fig. 3M). The shaft presents unordered and elongated pores with smoother areas in between (Fig. 3N). The distal end is weaker and covered by variable-sized pores which are sparsely distributed (Fig. 3O).

In **adults**, the proximal end is covered by isolated and closed pores that generate a smooth texture (Fig. 3P). Over the muscular scars, the texture becomes irregular and presents dimples. In the shaft, the texture is homogeneously smooth and silky (Fig. 3Q), and at the distal end, the surface is irregular by the presence of several muscular scars (Fig. 3R).
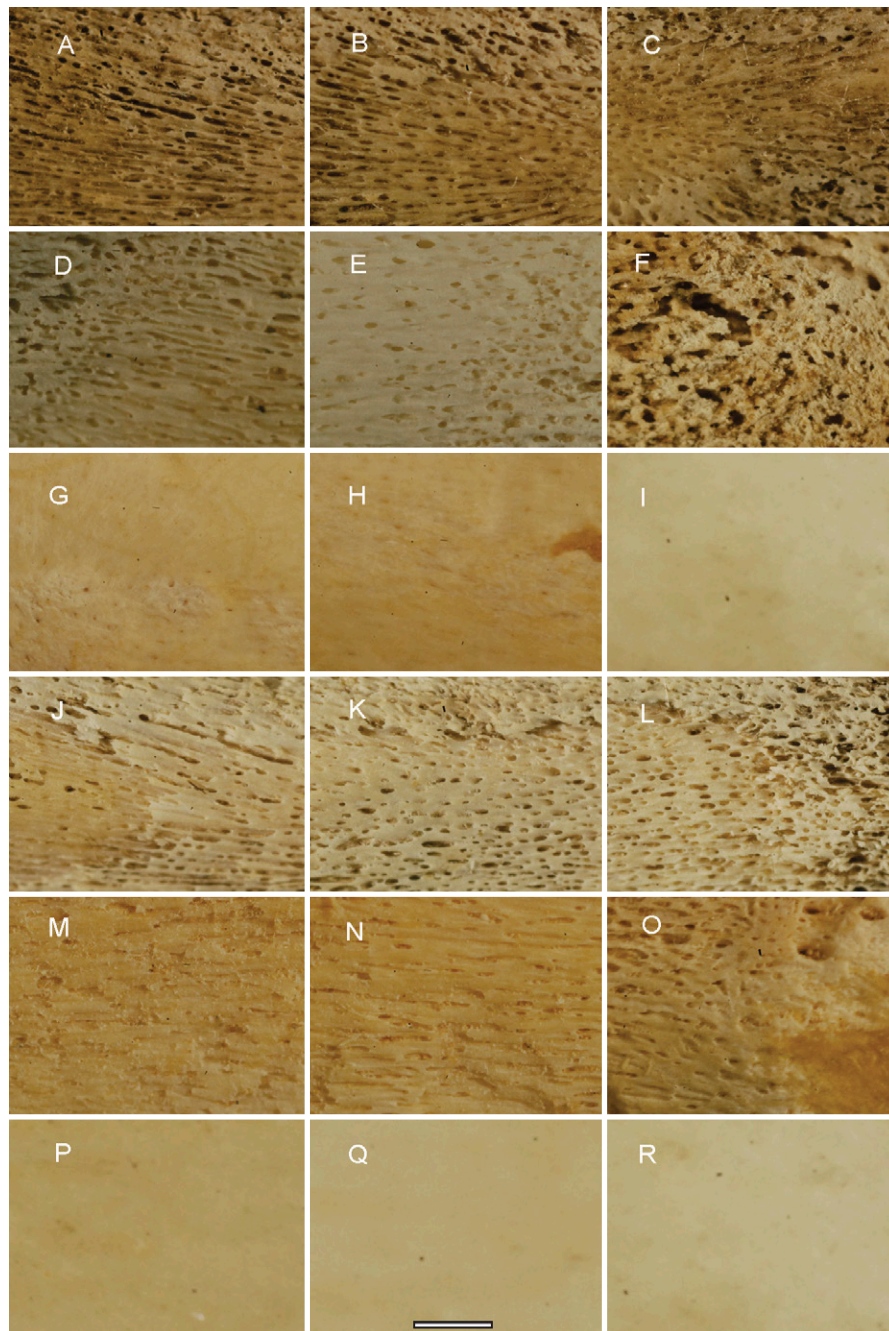
Fig. 4. Ulna textures in chicks (A−C, J−L), juveniles (D−F, M−O), and adults (D−F, P−Q). In all the cases, bones are oriented with the proximal end at the left: (A) proximal end in cranial view (MLP-O 810), (B) shaft in cranial view (MLP-O 810), (C) distal end in cranial view (MLP-O 817), (D) proximal end in cranial view (MLP-O 791), (E) shaft in cranial view (MLP-O 791), (F) distal end in cranial view (MLP-O 807), (G) proximal end in cranial view (MLP 470), (H) shaft in cranial view (MLP 687), (I) distal end in cranial view (MLP 687), (J) proximal end in caudal view (MLP-O 817), (K) shaft in caudal view (MLP-O 817), (L) distal end in caudal view (MLP-O 817), (M) proximal end in caudal view (MLP-O 806), (N) shaft in caudal view (MLP-O 806), (O) distal end in caudal view (MLP-O 807), (P) proximal end in caudal view (MLP 470), (Q) shaft in caudal view (MLP 470), (R) distal end in caudal view (MLP 470). Scale bar 1mm.

Ulna

Facies cranialis. In **chicks**, the proximal end exhibits areas more ossified than others. The outer layer of bone is very thin and presents grooves with pores arranged in sub-parallel rows that are more irregularly oriented in other areas (Fig. 4A). The shaft has elongated pores that converge forming longitudinal grooves, similar to those at the proximal and distal ends (Fig. 4B). The distal end presents also parallel grooves with pores irregularly distributed (Fig. 4C).

In **juveniles**, the proximal end is covered by small and sparse pores (Fig. 4D). In the transitional zone, the striations change the direction and become oblique to eventually disappear at the ends, where the surface is covered by small and sparse pores. The transitional zone,

toward the proximal end, presents large pores of variable shapes (*e.g.* rounded, elongated). Near to the articular area, pores are small, rounded, and sparse. The shaft has narrower striations and elongated pores (Fig. 4E). The *margo ventralis* is more striated, whereas the *margo dorsalis* is more porous. The distal end presents pores that merge forming larger holes (Fig. 4F).

In **adults**, the proximal end presents disperse and variable-sized pores irregularly distributed (Fig. 4G). Along the shaft (Fig. 4H), some dimples are more elongated, although most of the surface is smooth. Rounded and large dimples appear also in the *margo ventralis*, small pores and fine striations dorso-ventrally arranged are in the middle of the shaft. Tiny foramina aligned in finer stretch marks are observed in the *margo dorsalis*. At the distal end, the texture is homogeneously smooth (Fig. 4I).

Facies caudalis. In the **chicks**, this surface has a proximal end with sub-parallel furrows that bear elongated pores irregularly distributed (Fig. 4J). The density of the pores varies in each zone and among the specimens. Different textures are recognized in the shaft, where some areas are covered by wide grooves, and others have elongated pores irregularly distributed (Fig. 4K). The distal end is similar, although irregularly textured, with narrower and sub-parallel furrows and elongated pores (Fig. 4L). A thin layer of bone ossifies in patches, and the texture becomes smoother and not striated.

In **juveniles**, the proximal end is a little more ossified, and furrows are closed by a bony layer (Fig. 4M), like in the shaft (Fig. 4N). At the distal end, the texture becomes irregular by the presence of muscular scars, and the furrows are wider and sub-parallel (Fig. 4O).

In **adults**, the texture is completely smooth and homogenous along all the surface. The proximal end presents some isolated and small pores (Fig. 4P), which are absent in the shaft (Fig. 4Q), and weakly developed in the distal end (Fig. 4R).

Radius

Facies cranialis. In **chicks**, the proximal end presents oblique and slender grooves with elongated and rounded pores (Fig. 5A). Wide furrows distributed without a clear pattern and isolated dimples appear toward the shaft, besides a few oval pores (Fig. 5B). In MLP-O 787, a transitional zone between the shaft and the ends is characterized by elongated and dimples and wide furrows. The distal end is similar to the shaft (Fig. 5C). MLP-O 787 has wide furrows with a few pores on the entire surface, whereas MLP-O 796 does not present pores. MLP-O 805 lacks furrows but presents pores that vary laterally from rounded to elongated shapes

In **juveniles**, the proximal end presents a more ossified structure. The furrows are narrower and disposed closer to each other. Elongated and small pores are scattered, without any established pattern (Fig. 5D). The shaft presents parallel, tight striations and elongated

pores (Fig. 5E). The distal end exhibits a more irregular pattern, with pores of different sizes and some areas where the outer layer of bone is not completely ossified (Fig. 5F).

In **adults**, both ends are similarly textured. The proximal one presents a fibrous surface with some large and opened dimples (Fig G), which are different sized in MLP 687, and absent in MLP 470. The shaft is smoother (Fig. 5H) and without dimples, and the distal end is fibrous and presents small and scattered pores (Fig. 5I).

Facies caudalis. In **chicks**, the proximal end presents narrow and oblique furrows with small pores. The ossification varies in some areas and results in shallow depressions with wider furrows (Fig. 5J). However, MLP-O 805 presents a smoother surface with weak or lacking striations. The rest of the surface is similarly textured, the shaft (Fig. 5K), and the distal end (Fig. 5L) also present oblique and narrow furrows.

In **juveniles**, the proximal and distal ends are similarly textured. In the proximal end, dimples are densely distributed and furrows are not aligned (Fig. 5M). The shaft exhibits narrow and deep furrows longitudinally arranged with scattered pores (Fig. 5N). The distal end has small and dense pores (Fig. 5O).

The **adults** present a proximal end with a fibrous surface and interspersed silky areas (Fig. 5P). The shaft is smoother and silky, without pores and dimples (Fig. 5Q), and the distal end presents also a fibrous texture without any other surficial structure (Fig. 5R).

Carpometacarpus

Facies cranialis. In **chicks,** the proximal end is weakly ossified, and the thin bone layer that covers other areas in this bone is lacking. Short and wide furrows cover the surface (Fig. 6A). The shaft is covered by elongated pores that converge forming longitudinal wide grooves (Fig. 6B) that converge toward the ends in MLP-O 810. At the distal end, the elongated pores intersperse with deep furrows (Fig. 6C).

In **juveniles,** the proximal end presents rounded to elongated and isolated pores (Fig. 6D). The three metacarpals present a different texture in the middle part of the bone, with striations and elongated pores irregularly distributed in the metacarpal major (Fig. 6E). Narrower stretch marks and smaller pores are in the metacarpal minor. The alular metacarpal is smoother, without striations and with pores irregularly distributed. The distal end presents wide furrows and rounded small and pores (Fig. 6F).

In **adults**, the proximal end is slightly textured and not silky. Isolated oval foramina of different sizes are dispersed on this surface (Fig. 6G). In the middle part of the shaft, the surface is covered by a barely noticeable homogeneously distributed foramina (Fig. 6H).

Facies caudalis. In **chicks**, this surface is similar to the cranial one, with a proximal end covered by wide and
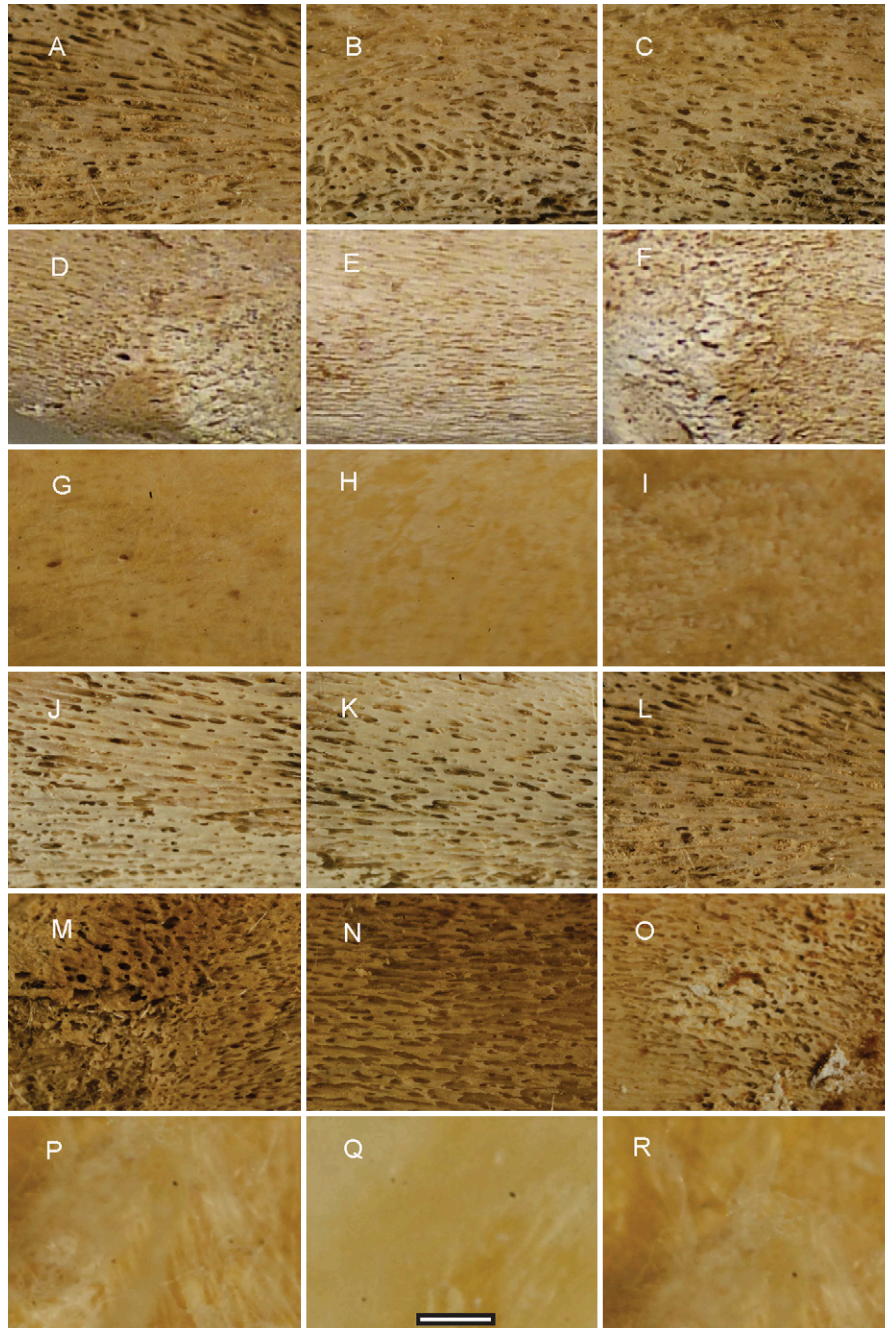
Fig. 5. Radius textures in chicks (A−C, J−L), juveniles (D−F, M−O), and adults (D−F, P−Q). In all the cases, bones are oriented with the proximal end at the left: (A) proximal end in cranial view (MLP-O 810), (B) shaft in cranial view (MLP-O 810), (C) distal end in cranial view (MLP-O 810), (D) proximal end in cranial view (MLP-O 791), (E) shaft in cranial view (MLP-O 791), (F) distal end in cranial view (MLP-O 791), (G) proximal end in cranial view (MLP 687), (H) shaft in cranial view (MLP 687), (I) distal end in cranial view (MLP 687), (J) proximal end in caudal view (MLP-O 817), (K) shaft in caudal view (MLP-O 817), (L) distal end in caudal view (MLP-O 817), (M) proximal end in caudal view (MLP-O 807), (N) shaft in caudal view (MLP-O 807), (O) distal end in caudal view (MLP-O 806), (P) proximal end in caudal view (MLP 470), (Q) shaft in caudal view (MLP 470), (R) distal end in caudal view (MLP 470) Scale bar 1 mm.

open furrows with elongated pores (Fig. 6J). The shaft presents elongated and large pores that merge constituting short furrows (Fig. 6K). The distal end exhibits depressed and less ossified areas with irregular and large pores (Fig. 6L).

In **juveniles**, the proximal end is covered by rounded and shallow pores irregularly distributed (Fig. 6M), whereas the shaft presents narrow furrows with elongat-ed pores (Fig. 6N). The distal end is similar to the middle area of the bone, with narrow furrows and elongated pores (Fig. 6O).

In **adults**, the surface is smoother. The proximal end is smooth and silky (Fig. 6P), whereas the shaft is smooth and bright (Fig. 6Q). The distal end presents also a smooth and silky surface, but covered by disperse and tiny foramina (Fig. 6R).
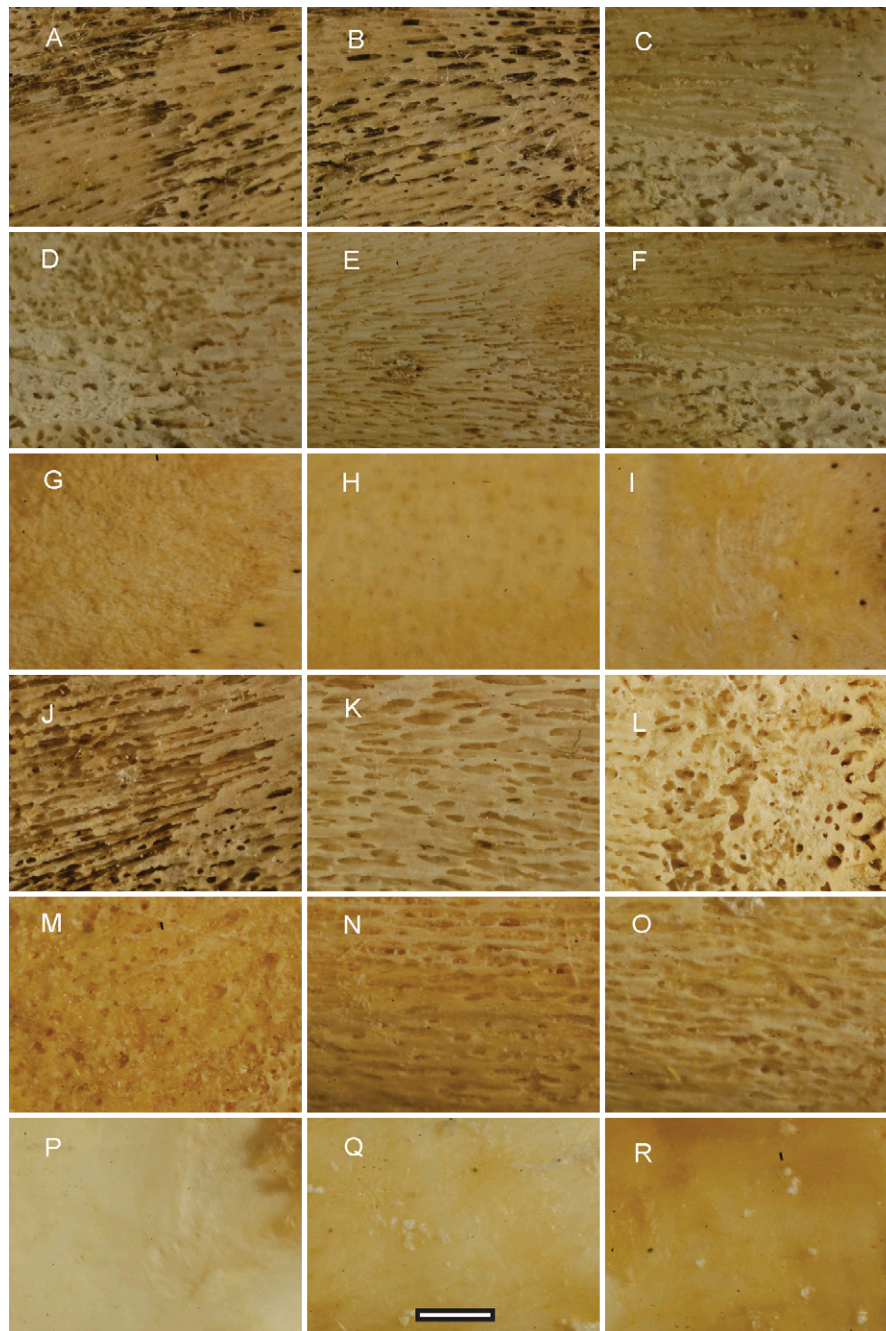
Fig. 6. Carpometacarpus textures in chicks (A–C, J–L), juveniles (D–F, M–O), and adults (D–F, P–Q). In all the cases, bones are oriented with the proximal end at the left: (A) proximal end in cranial view (MLP-O 810), (B) shaft in cranial view (MLP-O 810), (C) distal end in cranial view (MLP-O 807), (D) proximal end in cranial view (MLP-O 791), (E) shaft in cranial view (MLP-O 791), (F) distal end in cranial view (MLP-O 791), (G) proximal end in cranial view (MLP 687), (H) shaft in cranial view (MLP 687), (I) distal end in cranial view (MLP 470), (J) proximal end in caudal view (MLP-O 807), (K) shaft in caudal view (MLP-O 807), (L) distal end in caudal view (MLP-O 807), (M) proximal end in caudal view (MLP-O 807), (N) shaft in caudal view (MLP-O 807), (O) distal end in caudal view (MLP-O 791), (P) proximal end in caudal view (MLP 470), (Q) shaft in caudal view (MLP 470), (R) distal end in caudal view (MLP 470). Scale bar 1 mm.

Femur

Facies cranialis. In **chicks,** the proximal end presents pores of variable sizes and oblique furrows that disappear toward the lateral and medial sides, where the texture is porous and homogenous (Fig. 7A). The furrows of MLP-O 796 are closer and shallower than in the other specimens. The shaft is completely covered by large and irregular pores (Fig. 7B). A homogeneous and porous surface appears in MLP-O 805, whereas depressed areas comprising lagoons with pores within are observed in MLP-O 796. The distal end is similar to the proximal one, with irregular pores and oblique furrows. Two zones are separated by a diagonal line (Fig. 7C). The dorsal one is clearer, and the density of the pores is low. Some larger foramina are interspersed without any apparent
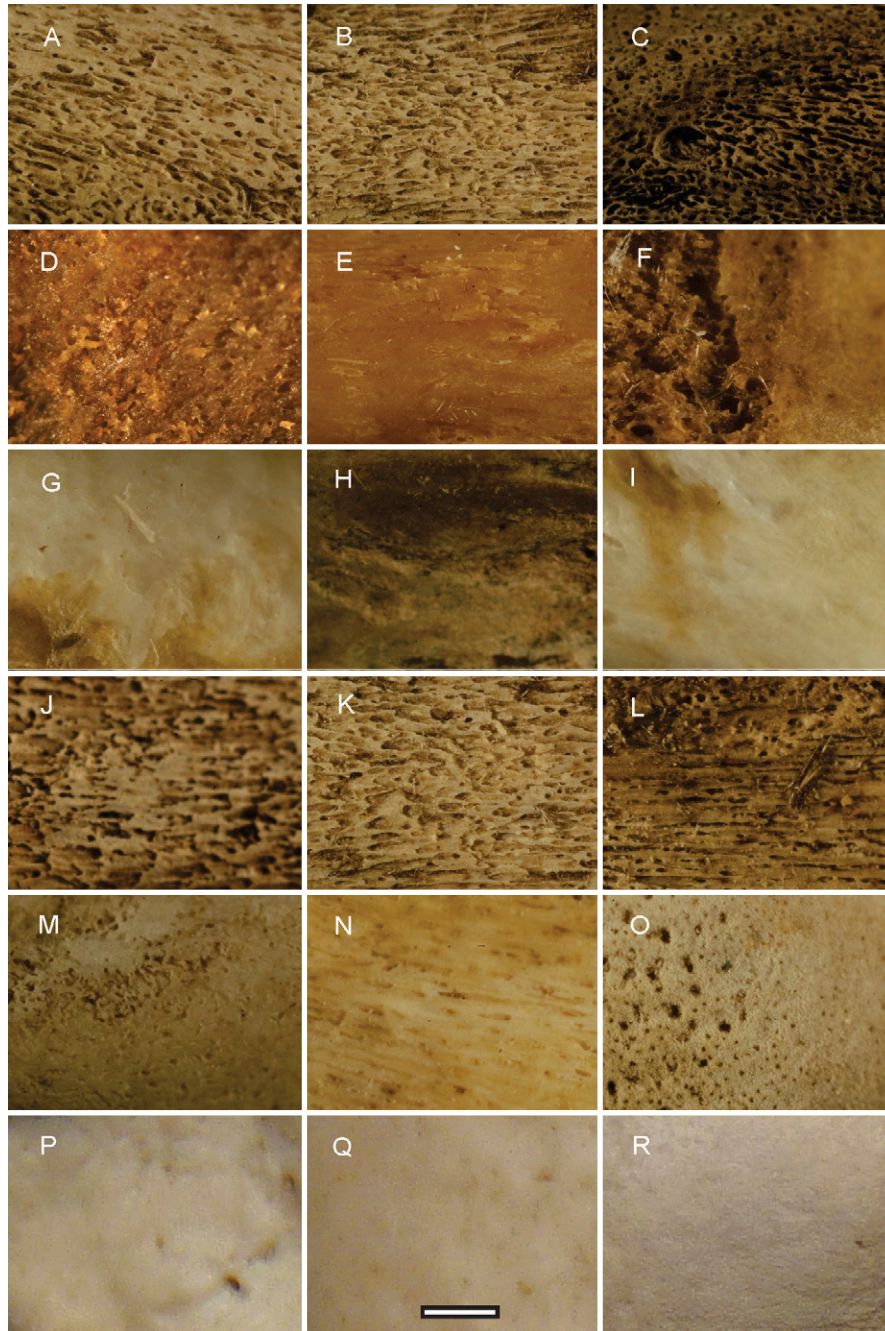
Fig. 7. Femur textures in chicks (A−C, J−L), juveniles (D−F, M−O), and adults (D−F, P−Q). In all the cases, bones are oriented with the proximal end at the left: (A) proximal end in cranial view (MLP-O 810), (B) shaft in cranial view (MLP-O 810), (C) distal end in cranial view (MLP-O 807), (D) proximal end in cranial view (MLP-O 791), (E) shaft in cranial view (MLP-O 791), (F) distal end in cranial view (MLP-O 791), (G) proximal end in cranial view (MLP 470), (H) shaft in cranial view (MLP 470), (I) distal end in cranial view (MLP 470), (J) proximal end in caudal view (MLP-O 787), (K) shaft in caudal view (MLP-O 787), (L) distal end in caudal view (MLP-O 787), (M) proximal end in caudal view (MLP-O 791), (N) shaft in caudal view (MLP-O 791), (O) distal end in caudal view (MLP-O 791), (P) proximal end in caudal view (MLP 470), (Q) shaft in caudal view (MLP 470), (R) distal end in caudal view (MLP 470). Scale bar 1 mm.

pattern. The ventral zone develops more elongated pores distributed with a higher density. Larger dimples might correspond to vascular foramina. Lateral variations are observed in the lattice of pores, whereas MLP-O 796 has a less ossified surface with small pores and thin walls.

In **juveniles**, the proximal end is irregularly textured, without pores and furrows (Fig. 7D). Pores only appear in the articular area. In the shaft, the texture is weakly striated around the *linea intermuscularis cranialis* (Fig. 7E). Shallow and isolated stretch marks become stronger at the level of the *crista supracondylaris medialis*. The surface is smooth on the *crista trochanterica* and the *facies articularis antitrochanterica*. The distal end presents different areas, one with a smooth surface, and another with pores homogeneously distributed on both condyles (Fig. 7F).

In **adults**, the texture of the whole surface is homogenous. The proximal end is silky and smooth (Fig. 7G), and comparatively, the shaft (Fig. 6R) is slightly fibrous with isolated and well-defined dimples (Fig. 7H). The distal end is also slightly fibrous, but dimples and other structures are absent (Fig. 7I).

Facies caudalis. In **chicks**, the surface presents irregular striations aligned with the axis of the bone, with pores and open furrows (Fig. 7J) in different areas toward the shaft that also presents elongated pores (Fig. 7K). The distal end presents strong striations and pores opening on the longitudinal crests between the stretch marks(Fig. 7L). These structures characterize all the faces of most of the specimens, whereas furrows of irregular distribution appear in MLP-O 805 and MLP-O 796. Pores are larger and denser than in the shaft of most specimens, but they are absent in MLP-O 805 and MLP-O 796.

In **juveniles**, there is a heterogeneous texture and the proximal end presents areas with a lattice of small pores and others with a smoother texture (Fig. 7M). The shaft presents narrow striations (Fig. 7N), and the distal end has some areas with pores of variable sizes and others with a surface homogeneously porous (Fig. 7O).

In **adults** the texture is smooth, and the proximal end presents few and isolated dimples (Fig. 7P). The shaft is smoother (Fig. 7Q) and the distal end is weakly rough (Fig. 7R).

Tibiotarsus

Facies cranialis. In **chicks,** the proximal end presents longitudinal rows of pores separated by furrows (Fig. 8A), a thin bony layer with fine striations appear as lateral variations. Pores are absent in MLP-O 805. The shaft has a more ossified compact bone with narrow and tight striations and irregular depressions (Fig. 8B). The distal end presents slender striations and pores uniformly distributed, particularly within the *sulcus extensorius* and the *incisura intercondylaris*, which are poorly developed (Fig. 8C). Pores are densely spread and combined with furrows in some areas.

In **juveniles,** both ends are similarly textured (Figs. 8D,F). The proximal end presents a well-defined striation with large and oval dimples (Fig. 8D). The shaft is smoother and develops a weak and tight striation (Fig. 8E). The distal end presents a porous surface, with openings of a variable size (Fig. 8F).

In **adults**, the proximal end is smooth and silky (Fig. 8G). In the shaft, the surface is silkier and without any other structure (Fig. 8H), and in the distal end the texture is homogeneously rough (Fig. 8I).

Facies caudalis. In **chicks**, the proximal end presents oblique furrows and different kinds of pores, some of them are large and elongated, but others are small and sub-rounded (Fig. 8J). The shaft presents variable-sized pores irregularly distributed, even in some depressed areas (Fig. 8K). Narrow and shallow furrows are present only in the *facies lateralis* and *medialis*. In the distal end, heterogeneous pores and narrow furrows are combined (Fig. 8L).

In **juveniles**, textures vary along the bone. The proximal end presents an irregular surface with small foramina and some other areas more ossified (Fig. 8M). Toward the *facies lateralis* and the *f. caudalis* of the shaft, furrows turn into fine wrinkles with tiny pores (Fig. 8N). In some other areas, the pores are absent. In the distal end, furrows are wider and shallower in some areas, whereas a few isolated pores open in others (Fig. 8O).

In **adults**, the proximal end presents weak and diffuse wrinkles (Fig. 8P), whereas the rest of the surface is smoother. The shaft is the silkier area (Fig. 8Q), while the distal end presents weak irregularities on the surface (Fig. 8R). In MLP 687 there are some obliterated and disperse pores.

Tarsometatarsus

Facies cranialis. In **chicks**, the proximal end has a striated surface, with narrow and tight furrows that converge toward the shaft (Fig. 9A). The shaft has wider furrows irregularly distributed with some areas with shallow depressions due to the poor ossification. Median pores irregularly distributed are combined with the furrows (Fig. 9B). In MLP-O 817 the texture is more homogenous and small pores are separated by well-defined walls. The distal end has deep and large pores of variable sizes (Fig. 9C).

In **juveniles**, the proximal and distal ends have smooth articular surfaces, covered by homogeneous foramina (Figs. 9D, F). In the proximal end, the *eminentia intercotylaris* (Fig. 9D) has fewer pores than the cotylae. The shaft presents a porous area with larger dimples with an irregular outline (Fig. 9E). Pores are also abundant in the *margo medialis*, and striations become more pronounced toward the trochlear end. Short furrows and elongated pores are only present in reduced areas (i.e. *margo lateralis*, on the lateral face of the trochlea IV, *sulci longitudinalis vascularia*). The distal end presents some areas with short and wide furrows, and others with an irregular porous surface (Fig. 9F).

In **adults**, the proximal end is irregular, the surface is smooth but with frequent and rounded dimples without any apparent pattern of distribution (Fig. 9G). The shaft is smoother and barely silky, with isolated and tiny pores (Fig. 9H). The distal end is completely smooth and silky, without pores or any other structure (Fig. 9I).

Facies caudalis. In **chicks**, the proximal end has elongated pores and areas with different relief due to the differences is the ossification of the outer layer (Fig. 9J). The shaft presents a homogeneous surface with variable pores, most of them of medium size (Fig. 9K). The distal end exhibits some areas with larger pores homogeneously distributed and other areas with more elongated pores (Fig. 9L).
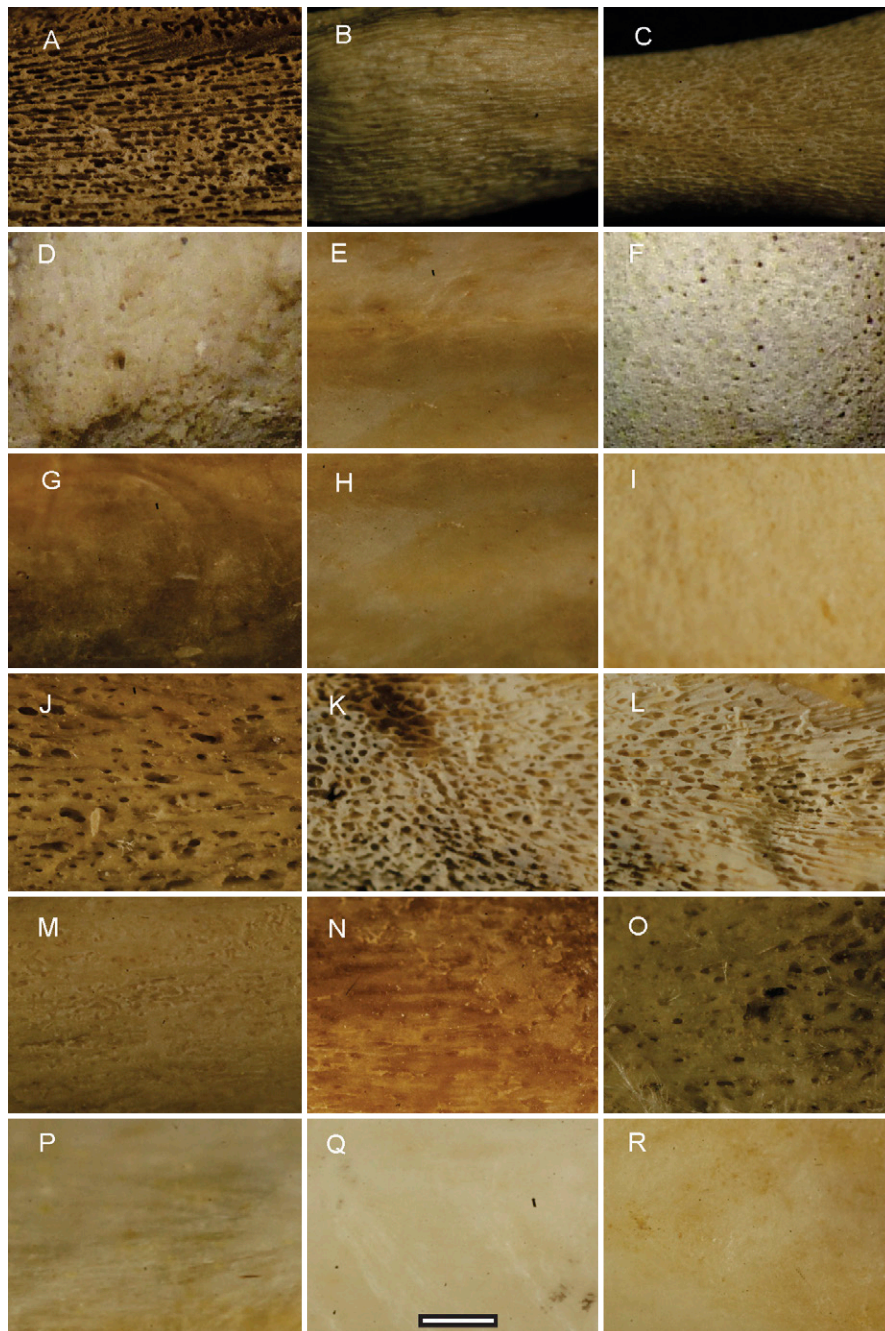
Fig. 8. Tibiotarsus textures in chicks (A−C, J−L), juveniles (D−F, M−O), and adults (D−F, P−Q). In all the cases, bones are oriented with the proximal end at the left: (A) proximal end in cranial view (MLP-O 810), (B) shaft in cranial view (MLP-O 790), (C) distal end in cranial view (MLP-O 790), (D) proximal end in cranial view (MLP-O 791), (E) shaft in cranial view (MLP-O 807), (F) distal end in cranial view (MLP-O 791), (G) proximal end in cranial view (MLP 470), (H) shaft in cranial view (MLP 470), (I) distal end in cranial view (MLP 470), (J) proximal end in caudal view (MLP-O 805), (K) shaft in caudal view (MLP-O 805), (L) distal end in caudal view (MLP-O 805), (M) proximal end in caudal view (MLP-O 791), (N) shaft in caudal view (MLP-O 791), (O) distal end in caudal view (MLP-O 791), (P) proximal end in caudal view (MLP 470), (Q) shaft in caudal view (MLP 470), (R) distal end in caudal view (MLP 470). Scale bar 1 mm.

In **juveniles**, in the proximal end, the cotylae are irregularly textured. The articular areas present a porous surface, whereas pores are smaller toward the shaft (Fig. 9M). In the shaft, the hypotarsus develops a smooth texture, with small and rounded pores densely distributed in restricted areas (Fig. 9N). In the distal end, the surface is homogeneously porous, only interrupted in a few smoother areas (Fig. 9O).

In **adults**, the proximal end has rounded and isolated dimples, although most of the surface is smooth (Fig. 9Q). The shaft present small pores distributed along all the surface (Fig. 9R), and the distal end represents the smoother and silkier area of the entire bone (Fig. 9S).
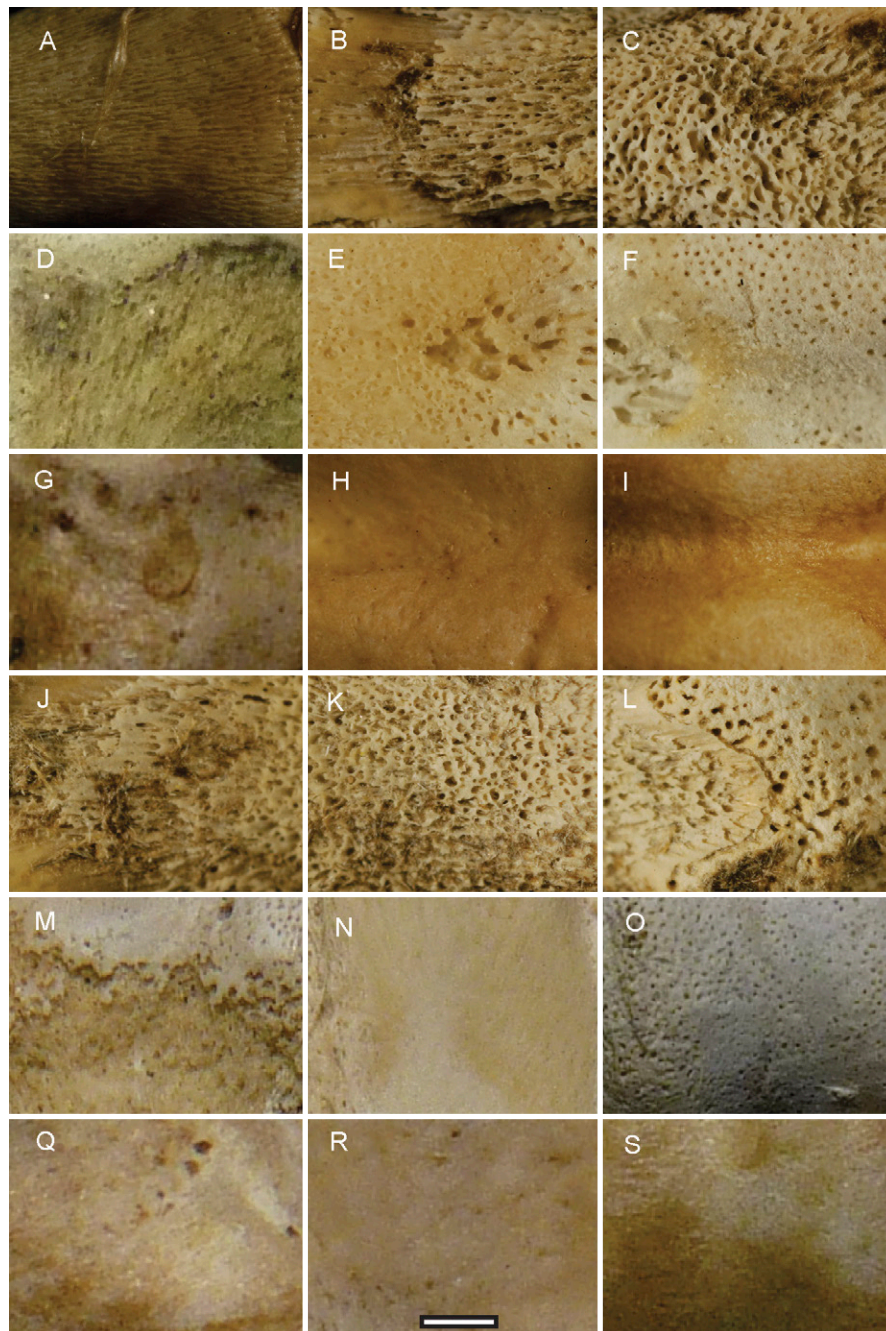
Fig. 9. Tarsometatarsus textures in chicks (A – C, J – L), juveniles (D – F, M – O), and adults (D – F, P – Q). In all the cases, bones are oriented with the proximal end at the left: (A) proximal end in cranial view (MLP-O 817), (B) shaft in cranial view (MLP-O 817), (C) distal end in cranial view (MLP-O 817), (D) proximal end in cranial view (MLP-O 791), (E) shaft in cranial view (MLP-O 807), (F) distal end in cranial view (MLP-O 791), (G) proximal end in cranial view (MLP 687), (H) shaft in cranial view (MLP 687), (I) distal end in cranial view (MLP 687), (J) proximal end in caudal view (MLP-O 790), (K) shaft in caudal view (MLP-O 790), (L) distal end in caudal view (MLP-O 790), (M) proximal end in caudal view (MLP-O 791), (N) shaft in caudal view (MLP-O 791), (O) distal end in caudal view (MLP-O 791), (P) proximal end in caudal view (MLP 470), (Q) shaft in caudal view (MLP 470), (R) distal end in caudal view (MLP 470). Scale bar 1 mm.

Discussion and conclusions

Determining the spectrum of variation in the bone texture in each ontogenetic stage, with the greatest precision, constitutes a useful tool for the analysis of birds collected in archaeological and paleontological sites. It gives us a new perspective for the understanding and in-

terpretation of these remains. We propose the first scale based on *Pygoscelis antarctica* for the recognition of the post-natal ontogenetic stages in penguins through a close examination of their bones. Regarding the stages and elements compared, our scale for penguins is equivalent to those already proposed and works as a complement of the scales known for Anatidae, Laridae, Ardeidae, Phalacrocoracidae, Procellariidae, and Alcidae (TUMARKIN-DE-

RATZIAN et al. 2006; WATANABE & MATSUOKA, 2013; ACOSTA HOSPITALECHE et al., 2017; WATANABE, 2017, 2018). It means, the present work deepens our knowledge about textural ageing in birds, adding the comparative context for Spheniscidae, a group that had not yet been analyzed from this perspective.

Chicks are represented by unfused and barely ossified elements, with ends not defined yet, and many elements indistinguishable from each other. Juveniles have more ossified bones, the youngest specimens within this category are slightly smaller than the adults, and the oldest ones reach the adult's size. The main difference between juveniles and adults is the texture of the superficial bone.

The textural bone of *Pygoscelis antarctica* shows a pattern of variation from chicks to adults, similar to that described for other birds (see TUMARKIN-DERATZIAN, 2006; WATANABE, 2018). In all these cases, the immature ages are characterized by the presence of porous, furrowed, and fibrous textures (TUMARKIN-DERATZIAN 2006; WATANABE 2018; this study). These textures are characteristics of a growing bone, consistent with a more vascularized osseous tissue, with channels opening to the bone surface through which blood and lymphatic vessels pass (TUMARKIN-DERATZIAN 2006; WATANABE 2018).

Beyond these common features, textures in chicks are slightly different in wings and legs. Bones of the wings are characterized by a shaft with wide furrows and large dimples, and both ends present elongated pores that join constituting short furrows. Patches of a thin and striated layer of bone cover the surface (Fig. 4L). In general, bones of the leg (Fig. 2) are a little more ossified than those of the wings (Fig. 1), and the thin layer of bone, observed as patches in the wing, appears in the legs as an almost continue layer (Fig. 8A). The elements of the legs have a shaft with isolated dimples, well-defined pores, and tight striations, whereas the ends have irregular striations aligned to the bone axis, and pores uniformly distributed.

These differences between the wing and legs texture might be related to the dissimilar demands of locomotion. Penguins are semi-altricial birds (STARCK & RICKLEFTS, 1998) that after hatching remain on the nest and depend on their parents to be fed. After a few days, chicks are able to use their legs to undertake excursions out of the nest, whereas the locomotion on water occurs later (BANNASCH, 1987). Studies in gulls (Laridae), whose chicks can walk a few days after hatching, showed that bones of the legs are more thick and resistant in early stages than those of the wings (CARRIER & LEON, 1990). Further analyses on bone structure and strength in penguins will be necessary to corroborate and expand these ideas.

Beyond these considerations, the main variability within the same stage was found in chicks, something that also happens in other aquatic birds (WATANABE, 2018). This is expected, due to the wider range of ages included in this category.

In juveniles, the ossification is indisputably greater predominating the presence of small pores opening in a smooth surface with scarce striations, mainly in the shaft. A similar pattern was found in the juveniles of other birds studied by WATANABE (2018). Unfortunately, a precise comparison with individuals of the same age of *Branta canadiensis* was not able due to differences in the definition of the ontogenetic stages; juveniles are treated as a category including all the individuals who are not sub-adults and adults (TUMARKIN-DERATZIAN, 2006). They describe a porous or fibrous texture without distinctions between younger and older specimens within juveniles. The texture we observed in juveniles indicates a decrease in vascularization and therefore, a diminution in bone growth rate (see WATANABE, 2018 and literature cited therein).

In adults, the smooth texture is consistent with matured osseous tissue, without channels and pores due to the absence of vascular tissues in the cortical layer (TUMARKIN-DERATZIAN 2006; WATANABE 2018; this study). Adults show less variability in textures and are characterized by bones with a smoother surface, silky or rough but with small and scattered pores, or rarely with narrow striations.

Some differences were observed between the ossification patterns of *Pygoscelis antarctica* and other birds, especially in the non-adult stages. For instance, chicks of *P. antarctica* have a humerus characterized by the presence of elongated pores and wide furrows in the shaft, with larger pores and furrows at the ends. Contrarily, in the rhinoceros auklet, *Cerorhinca monocerata*, the humerus is characterized by pores and a fibrous pattern in the shaft, and striations at the ends (WATANABE, 2018).

In summary, textural ageing once again demonstrated its methodological value for the assignment of isolated bones to each ontogenetic stage. However, the comparison between the textures described in the previous (TUMARKIN- DERATZIAN et al., 2006; WATANABE & MATSUOKA, 2013; WATANABE, 2018) and present contributions show a significant variation among taxonomic groups and between bones.

Definitively, the success of this method depends on the chosen proxy. For that reason, we are strongly convinced that it is necessary to perform this kind of comparative analysis in different families of birds to generate a more comprehensive database. This will allow making reliable ontogenetic assignments for each group of birds, minimizing the extrapolation of data.

Acknowledgments

References

Acosta Hospitaleche, C. (2004). *Los pingüinos* (*Aves, Sphenisciformes*) *fósiles de Patagonia. Sistemática, biogeografía y evolución*. Unpublished Ph. D. Dissertation, Facultad de Ciencias Naturales y Museo-Universidad Nacional de La Plata.

Acosta Hospitaleche, C. (2006). Taxonomic Longevity in Penguins (Aves, Spheniscidae). *Neues Jahrbuch für Geologie und Paläontologie*, **241**, 383–403.

Acosta Hospitaleche, C., Reguero, M. & Santillana, S. (2017). *Aprosdokitos mikrotero* gen. et sp. nov., the tiniest Sphenisciformes that lived in Antarctica during the Paleogene. *Neues Jahrbuch für Geologie und Paläontologie*, **283**, 25–34.

Bannasch, R. (1987) Morphologisch-funktionelle Untersuchung am Lokomotionsapparat der Pinguine als Grundlage für ein allgemeines Bewegungsmodell des „Unterwasserfluges". *Jahrbuch für Morphologie und mikroskopische Anatomie, 1. Abteilung*, **133**, 39–59.

Bannasch, R. (1994) How flipper-bands impede penguin swimming p. 28 *in*: Fraser R. & Trivelpiece, W. Z. (eds) *Report: Workshop on Seabird–Researcher Interactions*. Washington, DC, Office of Polar Programs.

Baumel, J. J. & Witmer, L. M. (1993). Osteologia, pp. 45–132 *in*: Baumel, J. J., King, S. A., Breazile, J. E., Evans, H. E. & Berge, J. C. (eds) *Handbook of Avian Anatomy: Nomina anatomica avium*. Cambridge, MA, Publications of the Nuttall Ornithological Club.

Cane, W. P. (1993). The ontogeny of postcranial integration in the common tern, *Sterna hirundo*. *Evolution*, **47**, 1138–1151.

Carrier, D. & Leon, L. R. (1990). Skeletal growth and function in the California gull (Larus californicus). *Journal of Zoology*, **222**, 375–389.

de Margerie, E. D., Robin, J. P., Verrier, D., Cubo, J., Groscolas, R. & Castanet, J. (2004). Assessing a relationship between bone microstructure and growth rate: a fluorescent labelling study in the king penguin chick (*Aptenodytes patagonicus*). *Journal of Experimental Biology*, **207**, 869–879.

Fujioka, T. (1955). Time and order of appearance of ossification centers in the chicken skeleton. *Acta Anatomica Nipponica*, **30**, 140–150.

Hogg, D. A. (1980). A re-investigation of the centres of ossification in the avian skeleton at and after hatching. *Journal of Anatomy*, **130**, 725.

Houssaye, A. (2009). "Pachyostosis" in aquatic amniotes: a review. *Integrative Zoology*, **4**, 325–340.

Knoll, F., Chiappe, L. M., Sanchez, S., Garwood, R. J., Edwards, N. P., Wogelius, R. A., ... & Marugán-Lobón, J. (2018). A diminutive perinate European Enantiornithes reveals an asynchronous ossification pattern in early birds. *Nature Communications*, **9**, 1–9.

Müller, G. B. & Streicher, J. (1989). Ontogeny of the syndesmosis tibiofibularis and the evolution of the bird hindlimb: a caenogenetic feature triggers phenotypic novelty. *Anatomy and Embryology*, **179**, 327–339.

Picasso, M. B. (2012). Postnatal ontogeny of the locomotor skeleton of a cursorial bird: greater rhea. *Journal of Zoology*, **286**, 303–311

Picasso, M. B. & Barbeito, C. G. (2018). Hindlimb bone maturation during postnatal life in the Greater Rhea (*Rhea americana*, Aves, Palaeognathae): Implications for palaeobiologibbcal and zooarchaeological interpretations. *Anatomia, Histologia, embryologia*, **47**, 398–404.

Piro, A. & Acosta Hospitaleche, C. (2019). Skull morphology and ontogenetic variation of the southern giant petrel *Macronectes giganteus* (Aves: Procellariiformes). *Polar Biology*, **42**, 27–45.

Pourlis, A. F., Magras, I. N. & Petridis, D. (1998). Ossification and growth rates of the limb long bones during the prehatching period in the quail (*Coturnix coturnix japonica*). *Anatomia, Histologia, Embryologia*, **27**, 61–63.

Pourlis, A. F. & Antonopoulos, J. (2014). The ossification of the pelvic girdle and leg skeleton of the quail (*Coturnix coturnix japonica*). *Anatomia, Histologia, Embryologia*, **43**, 294–300.

Rogulska, T. (1962). Differences in the process of ossification during the embryonic development of the chick (*Gallus domesticus* L.), rook (*Corvus frugilegus* L.) and black-headed gull (*Larus ridibundus* L.). *Zoologica Poloniae*, **12**, 223–236.

Sosa, M. A. & Acosta Hospitaleche, C. (2018). Ontogenetic variations of the head of *Aptenodytes forsteri* (Aves, Sphenisciformes): muscular and skull morphology. *Polar Biology*, **41**, 225–235.

Starck, J. M. (1993). Evolution of avian ontogenies, pp. 275–366 *in*: Power, D.M. (ed.) *Current Ornithology 10*. New York, NY, Plenum Press.

Starck, J. M. & Ricklefs, R. (1998). Patterns of development: the altricial-precocial spectrum, pp. 3–30 *in*: Starck, J. M. & Ricklefs, R. (eds) *Avian Growth and Development, Evolution between the Altricial-Precocial Spectrum*. New York, NY, Oxford University Press.

Tumarkin-Deratzian, A. R., Vann, D. R. & Dodson, P. (2006). Bone surface texture as an ontogenetic indicator in long bones of the Canada goose *Branta canadensis* (Anseriformes: Anatidae). *Zoological Journal of the Linnean Society*, **148**, 133–168.

Watanabe, J. (2017). Ontogeny of macroscopic morphology of limb bones in modern aquatic birds and their implications for ontogenetic ageing, pp. 183–220 *in*: Acosta Hospitaleche, C., Agnolin, F., Haidr, N., Noriega, J. I. & Tambussi, C. P. (eds) *Paleontología y Evolución las Aves*. Buenos Aires, Museo Argentino de Ciencias Naturales "Bernardino Rivadavia".

Watanabe, J. (2018). Ontogeny of surface texture of limb bones in modern aquatic birds and applicability of textural ageing. *Anatomical Record*, **301**, 1026–1045

Watanabe, J. & Matsuoka, H. (2013). Ontogenetic change of morphology and surface texture of long bones in the gray heron (*A. cinerea*, Ardeidae), pp. 279–306 *in*: Gohlich, U. B. & Kroh, A. (eds) *Paleornithological Research 2013*: *Proceedings of the 8th International Meeting of the Society of Avian Paleontology and Evolution*. Vienna, Naturhistorisches Museum Wien.

Waterston, D. & Geddes, A. C. (1910). X. Report upon the Anatomy and embryology of the penguins collected by the Scottish National Antarctic Expedition, comprising: (1) Some features in the anatomy of the penguin;(2) The embryology of the penguin: a study in embryonic regression and progression. *Earth and Environmental Science Transactions of the Royal Society of Edinburgh*, **47**, 223–244.